



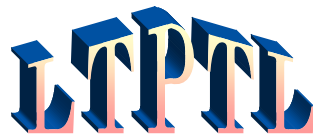
Low Temperature Plasma Technology Laboratory

Equilibrium theory for plasma discharges of finite length

Francis F. Chen and Davide Curreli

LTP-1106

June, 2011



Electrical Engineering Department
Los Angeles, California 90095-1594

Equilibrium theory for plasma discharges of finite length

Francis F. Chen¹ and Davide Curreli^{1,2}

¹University of California, Los Angeles, California 90095-1594

²University of Padua, Padua, Italy

ABSTRACT

Partially ionized plasmas, often driven by radiofrequency power, are commonly used in semiconductor manufacturing. Their equilibrium distributions of density, temperature, and even distribution functions, have been modeled by PIC simulations, but only one case at a time, and with disregard for the sheath boundary conditions. Analytic theory fails to predict the observed density profiles $n(r)$, especially in the presence of a dc magnetic field \mathbf{B} . To gain insight into the physics, we adopt a simple 1-D model: a cylinder of intermediate length bounded by sheaths on the endplates. We find that a short-circuit effect allows the electrons to follow the Boltzmann relation even across \mathbf{B} . This assumption leads to a simple nonlinear equation for the ion drift velocity, whose solution gives density profiles that are quite generally peaked on axis and naturally match to the Debye sheath on the sidewalls. A code EQM is developed to solve this equation together with those for neutral depletion and local ionization balance. The solutions agree with experiment and throw light on the classic problems of anomalous skin depth and cross-field diffusion. Energy balance requires knowing the energy deposition. For this we use the HELIC code for helicon discharges. Iteration of EQM with HELIC yields not only all the radial profiles but also the absolute values of density and electron temperature.

The problem of anomalous skin depth was pointed out by Weibel¹, who proposed that thermal motions of electrons generated in the skin layer of an rf plasma can take them into the interior to produce ionization there. Data showing a center-peaked density profile $n(r)$ in a cylindrical Inductively Coupled Plasma (ICP) with an antenna wound on the perimeter are shown in Fig. 1. Density extends well beyond the rf field. Following Weibel, numerous papers using kinetic theory in plane geometry ensued; some were listed in a previous PRL². A stronger effect utilizing cylindrical geometry and the nonlinear Lorentz force was shown to agree better with experiment². By using a 1-D model involving a cylinder with endplates, we find that the anomaly can be explained simply by equilibrium conditions. When there is a dc \mathbf{B} -field, anomalous electron transport across \mathbf{B} has been a vexing problem in fully ionized fusion plasmas. In partially ionized gases, even the very earliest experiments on helicon discharges³ at $B \geq 0.075$ T showed axially peaked $n(r)$, though we now know⁴ that the rf energy deposition is mainly at the edge at those fields. Central to our theory are the sheath boundary conditions at the endplates, to be explained later, which permit an explanation of cross-field transport that is not available for fusion plasmas.

Guided by experiment, we reduce the problem to its essentials by assuming a cylindrical discharge of radius a and length L short enough that we can neglect gradients in the z (axial) direction. The coaxial \mathbf{B} -field is such that electron and ion gyroradii r_L are $\ll a$ and $\gg a$, respectively. The steady-state ion fluid equation of motion is

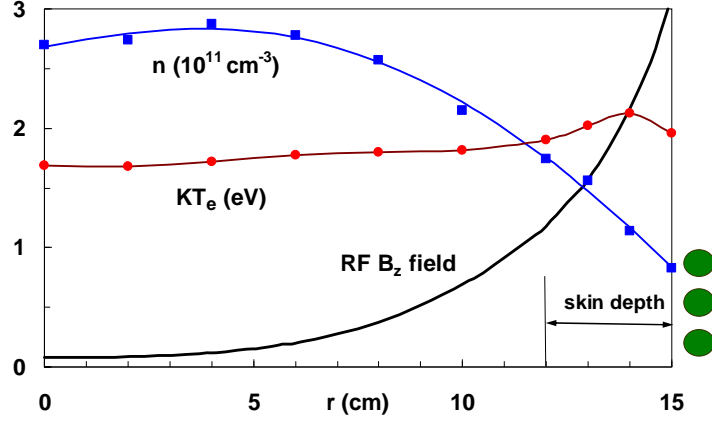


Fig. 1. Radial profiles² of n , KT_e , and rf B_z in an ICP with antenna elements only on the periphery, as shown. The density is peaked well outside the classical skin depth, though the electron temperature KT_e peaks in the skin.

$$M\mathbf{v}\nabla \cdot (n\mathbf{v}) + Mn\mathbf{v} \cdot \nabla \mathbf{v} = -en\nabla\phi + en(\mathbf{v} \times \mathbf{B}) - KT_i\nabla n - Mn\nu_{io}\mathbf{v}. \quad (1)$$

Here M is the ion mass, n the plasma density, \mathbf{v} the ion fluid velocity, ϕ the plasma potential, and ν_{io} the ion-neutral charge-exchange collision frequency. We consider a one-dimensional equilibrium in which the θ and z gradients are ignored. We assume $r_{Li} \gg a$ so that the $\mathbf{v} \times \mathbf{B}$ term can be ignored, and similarly the T_i term if $T_i \ll T_e$. The $\mathbf{v} \cdot \nabla \mathbf{v}$ term is from transforming from particle to fluid velocities⁵, and the $\nabla \cdot (n\mathbf{v})$ term accounts for ionization, which injects slow ions⁶. It will be convenient to define the ionization and collision probabilities P_i and P_c as:

$$P_i(r) \equiv \langle \sigma v \rangle_{ion}(r), \quad P_c(r) \equiv \langle \sigma v \rangle_{cx}(r) = \nu_{io} / n_n, \quad (2)$$

where n_n is the density of neutrals. P_c varies with $T_e(r)$, and P_i with the ion drift $v(r)$. The ion equation of continuity is

$$\nabla \cdot (n\mathbf{v}) = nn_n P_i(r), \quad (3)$$

which can be used in the first term of Eq.(1). With the usual normalizations $\eta \equiv -e\phi / KT_e$ and $c_s \equiv (KT_e / M)^{1/2}$, the radial component of Eq. (1) with $v \equiv v_r$ becomes

$$v \frac{dv}{dr} = c_s^2 \frac{d\eta}{dr} - n_n (P_c + P_i)v. \quad (4)$$

Eq. (3) can be written

$$\frac{dv}{dr} + v \frac{d(\ln n)}{dr} + \frac{v}{r} = n_n P_i(r). \quad (5)$$

We wish to show next that the electrons are Maxwellian even in a strong dc B-field. In a long plasma, electrons can be Maxwellian along each field line, but their densities can vary independently across field lines at low pressures when cross-field diffusion is slow. However, in discharges of finite length set by endplates which are not too far apart, adjustment of the endplate sheaths can cause the electron density to behave *as if* the electrons had moved across \mathbf{B} . This Simon short-circuit effect⁷ is shown in Fig. 2. Suppose ionization is high on the outside of the plasma and low on the inside. Consider two magnetic tubes, No. 1 with high density near the wall, and No. 2 with low density near the center. In tube 1, almost all electrons traveling toward the endplate are reflected by the sheath field, and the sheath drop adjusts so that the electron flux is equal to the ion flux to keep that tube quasineutral. In tube 2, the density is lower, so the ion

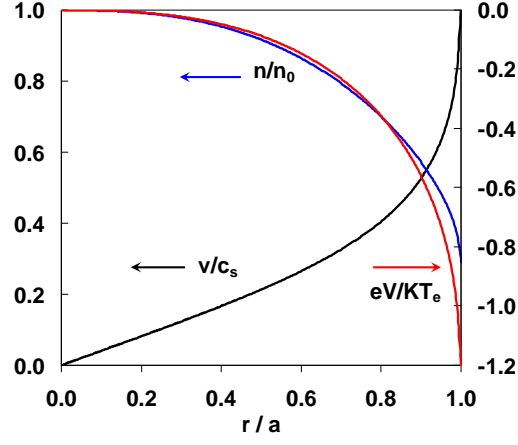


Fig. 3. Solution of Eq. (8) and associated equations for $KT_e = 3$ eV. These profiles do not change with tube radius a or pressure p but change with T_e , which affects the value of k .

Solution of Eq. (8) for constant k yields self-similar profiles for all discharges, magnetized or not, which satisfy our assumptions. If ρ is rescaled so that $v = c_s$ at $r/a = 1$, the profiles, shown in Fig. 3, are independent of the quantities n_n , P_i , and c_s in the definition of ρ as long as k constant. When T_e varies, the ratio P_c/P_i , and hence k , changes, and the profiles change somewhat; but the density profile is always centrally peaked, as shown in Fig. 3.

Note that the ion velocity is known at each radius, so that the variation of $P_c(r)$ is taken into account up to the sheath edge. No presheath needs to be assumed. Up to now, n_n and T_e have been given arbitrary constant values, but they are related by ionization balance. It is well known that, for ion creation to balance loss by diffusion, n_n and T_e must have an inverse relationship⁸. The local balance at each radius can be shown to give

$$\frac{1}{nr} \frac{d}{dr} (rnv) = n_n P_i(T_e). \quad (9)$$

If we solve Eqs. (7) and (9) simultaneously for a given discharge radius a , only one value of T_e at each pressure gives $v = c_s$ at a . Repeating this for different pressures yields $n_n - T_e$ curves for each value of a , with $P_c(r)$ evaluated with the local value of v . However, the true T_e depends on energy balance, which will be discussed later.

We now consider neutral depletion. If their mean free paths are sufficiently short, neutrals with temperature T_n and self-collision frequency ν_{nn} diffuse at the rate $n_n \nu_n = -D \nabla n_n$ with the coefficient $D = KT_n / M \nu_{nn}$. Since they are lost at the ionization rate, their equation of continuity for constant T_n is

$$D \nabla^2 n_n = n_n n P_i. \quad (10)$$

The boundary conditions are $\nabla n_n(0) = 0$ and $n_n \nu_n(a) = N_0 p_0 (KT_n / 2\pi M)^{1/2}$, where p_0 is the input pressure in mTorr and $N_0 = 3.3 \times 10^{13} \text{ cm}^{-3}$. We have devised a code EQM which solves Eqs. (7), (9), and (10) simultaneously using a fourth-order Runge-Kutta process for the integrations. Note that Eq. (7) is dimensional. Figure 4 gives an example of the plasma and density profiles for $n_0 = 10^{12} \text{ cm}^{-3}$, and Fig. 5 shows these at higher densities with extreme neutral depletion. We see that T_e rises to unreasonably high values as n_n drops. This is because

radiative losses have not yet been taken into account. To do this requires detailed knowledge of the energy input mechanism in a specific discharge.

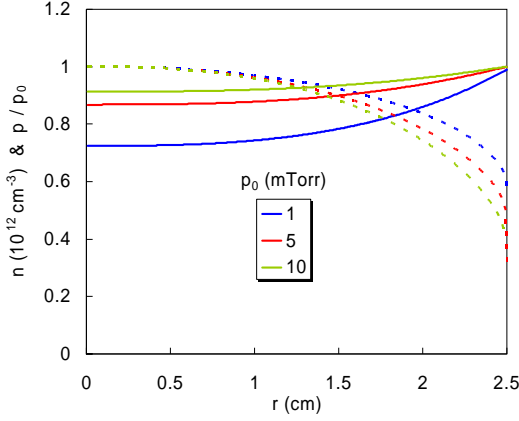


Fig. 4. Plasma density (solid) and neutral pressure profiles (dashed) for argon discharges in a 5-cm diam tube with $n_0 = 10^{12} \text{ cm}^{-3}$ and initial pressures $p_0 = 1, 5,$ and 10 mTorr at 400 K .

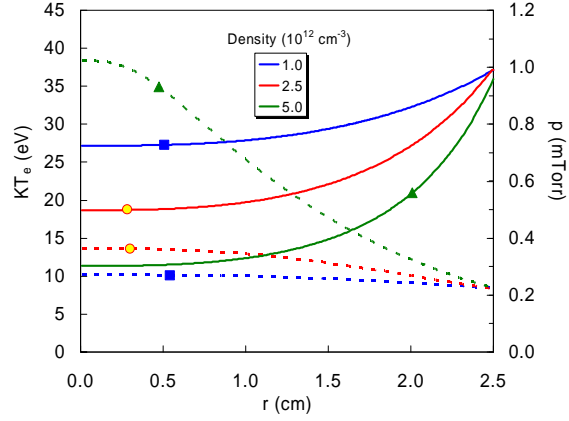


Fig. 5. Neutral pressure profiles in the same tube with $p_0 = 1 \text{ mTorr}$ and various peak plasma densities. The corresponding T_e profiles (dotted lines) are identified by the symbols.

For this, we have chosen the helicon discharge, for which the energy deposition profile can be computed with the HELIC code of Arnush⁴. The HELIC code can calculate the rf power deposition profile $P_{\text{rf}}(r)$ for a cylindrical discharge with endplates, uniform B-field, constant $n(z)$ and $n_n(z)$, and arbitrary profiles $n(r)$, $T_e(r)$, and $n_n(r)$. Various types of antennas can be assumed, and the absolute power into the plasma is specified by the antenna current. The energy lost by radiation before each ionization has been given as a function of T_e by Vahedi⁹. There is also a small loss due to particle fluxes to the walls and endplates. At high B-fields, energy deposition is peaked close to the wall by the Trivelpiece-Gould mode⁴. Energy balance is obtained by equating the rf energy input at each radius to the energy lost in ionization and radiation at that radius. This yields the absolute value of $T_e(r)$ and $n(r)$. The Boltzmann relation is now evaluated using the local T_e . The complete solution is obtained by iterating between the EQM and HELIC codes. Initially, EQM is solved with uniform ionization, giving $n(r)$, $T_e(r)$, and $n_n(r)$. These profiles are fitted with a 6-degree polynomial to be entered into HELIC to obtain $P_{\text{rf}}(r)$. Energy balance yields $T_e(r)$. This profile, representing nonuniform ionization, is then entered into EQM to obtain new profiles of n , T_e , and n_n . The process is repeated until it converges. It normally takes only five or six iterations for convergence. An example of such a solution is shown in Figs. 6 and 7.

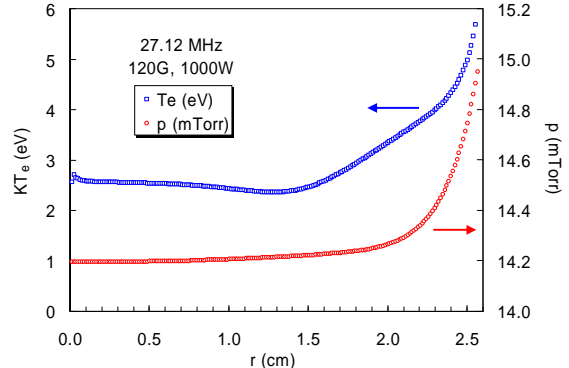
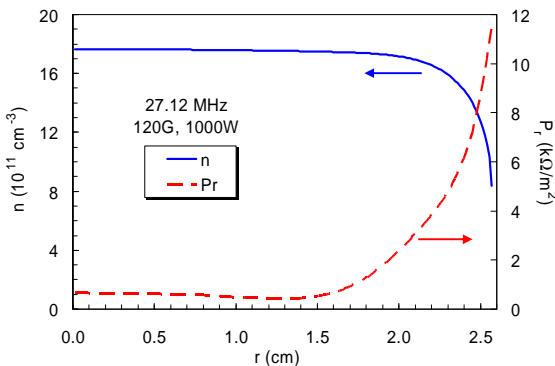


Fig. 6. Curves of $n(r)$ (—) and $P_{\text{rf}}(r)$ (- - -) (color online), obtained by iteration of EQM with HELIC, for a 15-mTorr helicon discharge at 120G with 1000W of rf at 27.12 MHz and an $m = 0$ antenna.

Fig. 7. Radial profiles of KT_e and neutral pressure p corresponding to the discharge in Fig. 6. Note that p (right scale) has a suppressed zero.

In summary, the short-circuit effect allows electrons to “move” across B-fields to follow the Boltzmann relation everywhere. In that case, simple equilibrium considerations explain the central peaking of density profiles observed in experiment without the need for complicated theories of anomalous skin depth or anomalous electron transport. In equilibrium, ions are driven radially outward by the E-field associated with the peaked density profiles. In units that depend weakly on plasma parameters, a universal density profile depending only on T_e is obtained which takes collisions into account exactly and matches to the Debye sheath without the need for a presheath assumption. Iteration with a helicon code yields absolute-value radial profiles of plasma density and electron temperature, including neutral depletion.

¹ E.S. Weibel, Phys. Fluids **10**, 741 (1967).

² J.D. Evans and F.F. Chen, Phys. Rev. Lett. **86**, 5502 (2001).

³ R.W. Boswell, Phys. Lett. **33A**, 457 (1970).

⁴ D. Arnush, Phys. Plasmas **7**, 3042 (2000).

⁵ F.F. Chen, *Introduction to Plasma Physics and Controlled Fusion*, 2nd ed., Vol. 1, p. 58ff. (Plenum Press, New York, 1984).

⁶ A. Fruchtman, G. Makrinich, and J. Ashkenazy, Plasma Sources Sci. Technol. **14**, 152 (2005).

⁷ A. Simon, Phys. Rev. **98**, 317 (1955).

⁸ M.A. Lieberman and A.J. Lichtenberg, *Principles of Plasma Discharges and Materials Processing*, 2nd ed. (Wiley-Interscience, Hoboken, NJ, 2005), p 334); F. F. Chen and J.P. Chang, *Principles of Plasma Processing* (Kluwer/Plenum, New York, 2002), p. 70ff.

⁹ V. Vahedi, *Modeling and simulation of rf discharges used for plasma processing*, Thesis, University of California, Berkeley (1993).